

AperTO - Archivio Istituzionale Open Access dell'Università di Torino

Hydrothermal dolomitization of the carbonate Jurassic succession in the Provençal-Dauphinois and Subbriançonnais Domains (Maritime Alps, North-Western Italy)

This is the author's manuscript

Original Citation:

Availability:

This version is available <http://hdl.handle.net/2318/130657> since

Published version:

DOI:10.1016/j.crite.2012.10.015

Terms of use:

Open Access

Anyone can freely access the full text of works made available as "Open Access". Works made available under a Creative Commons license can be used according to the terms and conditions of said license. Use of all other works requires consent of the right holder (author or publisher) if not exempted from copyright protection by the applicable law.

(Article begins on next page)



UNIVERSITÀ DEGLI STUDI DI TORINO

This is an author version of the contribution published on:

Questa è la versione dell'autore dell'opera:

Comptes Rendus Geoscience, Vol. 345, No. 1, pp. 47–53

(DOI: 10.1016/j.crte.2012.10.015)

The definitive version is available at:

La versione definitiva è disponibile alla URL:

<http://ees.elsevier.com/crgeoscience/>

1 **Hydrothermal dolomitization of the carbonate Jurassic succession in the Provençal and**
2 **Subbriançonnais Domains (Maritime Alps, North-Western Italy)**

3
4 *Dolomitisation hydrothermale de la succession carbonatée jurassique dans les zones Provençale*
5 *et Subbriançonnaise (Alpes Maritimes, Nord-Ouest de l'Italie)*

6 Luca Barale^{a*}, Carlo Bertok^a, Anna d'Atri^a, Gabriele Domini^b, Luca Martire^a and Fabrizio Piana^c

7
8 KEY WORDS. Hydrothermal dolomite, Provençal Domain, Maritime Alps, Jurassic limestones.

9 ABSTRACT. The present paper illustrates a straightforward case of hydrothermal dolomitization,
10 affecting Jurassic platform limestones of the Provençal and Subbriançonnais Domains (Maritime
11 Alps, North-Western Italy). Dolomitized bodies are randomly distributed within the host limestone,
12 and are commonly associated with dolomite vein networks and tabular bodies of dolomite-cemented
13 breccias discordant with respect to bedding. Main dolomite types are a finely to medium-crystalline
14 replacive dolomite and a coarsely crystalline saddle dolomite occurring both as replacive and as
15 cement. Stratigraphic constraints indicate that dolomitization occurred during the Cretaceous, in a
16 shallow burial context, and was due to the circulation of hot fluids (temperature about 200 °C, as
17 indicated by fluid inclusion microthermometry) through faults and related fracture networks.
18 Hydrothermal dolomitization therefore indirectly documents a Cretaceous fault activity in the
19 Maritime Alps segment of the European Tethyan passive margin.

20
21 MOTS CLÉS. Dolomite hydrothermale, Zone Provençale, Alpes Maritimes, calcaires jurassiques.

22 RÉSUMÉ. Cet article montre pour la première fois l'effet de dolomitisation hydrothermale sur des
23 séries jurassiques de plate-forme dans les zones Provençale et Subbriançonnaise (Alpes Maritimes,
24 Nord-Ouest de l'Italie). Les masses dolomitisées ont une distribution casuelle dans le calcaire hôte,
25 et sont communément associées avec réseaux de veines dolomitiques et corps tabulaires de brèches
26 à ciment dolomitique discordants par rapport à la stratification. Les typologies principales de
27 dolomite comprennent une dolomite de remplacement à grain fin à moyen et une dolomite en selle à
28 grain grossier. De fortes contraintes stratigraphiques indiquent que la dolomitisation a eu lieu dans
29 le Crétacé, dans des conditions d'enfouissement très superficielles. Cette dolomitisation était liée à
30 la circulation de fluides très chauds (environ 200 °C) à travers un réseau de failles et diaclases. La

^a Dipartimento di Scienze della Terra, Università di Torino, 10125 Torino, Italy.

^b Strada Marentino 2, 10020 Andezeno (TO), Italy.

^c CNR-IGG, Istituto di Geoscienze e Georisorse, unità di Torino, 10125 Torino, Italy.

* Corresponding author.

E-mail address: luca.barale@unito.it

31 dolomitisation hydrothermale est donc un argument indirect en faveur d'une activité tectonique
32 créacée dans les zones Provençale et Subbriançonnaise de la marge passive Européenne de la
33 Téthys Alpine.

34

35

36

37 **1. Introduction**

38

39 Among the many facets of the so called "dolomite problem" (see Machel, 2004, for discussion and
40 references), hydrothermal dolomite has been recently the object of interest and debate (Machel and
41 Lonnee, 2002; Davies and Smith, 2006). In order for dolomite to be interpreted as hydrothermal not
42 only a relatively high temperature of formation is to be proved but it should be coupled to inferred
43 burial depths that cannot justify the calculated temperatures, insofar suggesting the upward
44 advection of hot dolomitizing fluids (Machel, 2004).

45 In the stratigraphic successions of the Maritime Alps at the south-eastern termination of the
46 Argentera Massif, a dolomitization of the Jurassic limestones was reported by those authors who
47 dealt with these areas in the past decades (Campanino Sturani, 1967; Carraro et al., 1970; Malaroda,
48 1970) but neither detailed description nor attempts of interpretation were provided. Stratigraphic
49 constraints, geometry and petrography of the dolomitized bodies, and isotope data and fluid
50 inclusion microthermometry allow to reconstruct age, temperatures and burial depth for the
51 dolomite of the Jurassic succession of the study area

52 The purpose of this paper, therefore, is to contribute to refine the understanding of the
53 dolomitization process, by means of a case history, and, from a regional point of view, to evaluate
54 the implications of the occurrence of this kind of dolomite on the tectono-sedimentary evolution of
55 this part of the passive European Tethyan margin.

56

57 **2. Geographic and geological setting**

58

59 The study area is located in the north-eastern Maritime Alps (North Western Italy), between the
60 Sabbione Valley to the west and the upper Vermentina Valley to the east, close to the village of
61 Palanfrè (Fig. 1). This sector is composed of several tectonic units, presently superimposed along
62 low-angle NW-SE striking Alpine tectonic contacts. Their geometrical position has been classically
63 interpreted to reflect the paleogeographic position along the Mesozoic European paleomargin of the
64 western Tethys, thus the lowest units have been classically attributed to the more external

65 Dauphinois Domain, and the overlying units to the more internal Subbriançonnais Domain (Carraro
66 et al., 1970).

67 More precisely, in the study area the main features of the Dauphinois succession are closely
68 comparable to the Provençal ones, that are characterized by a reduced thickness and shallow water
69 facies. In the following, we will refer to this succession as Provençal. It starts with Permian
70 continental sediments that rest on the crystalline basement of the Argentera Massif and are
71 characterized by marked thickness changes; they are followed by some tens of meters of Lower
72 Triassic coastal siliciclastic deposits and Middle Triassic peritidal dolomitic limestones. A regional
73 discontinuity surface corresponding to a Late Triassic-Middle Jurassic hiatus is followed by a thick
74 (200-300 m) succession of Middle?-Upper Jurassic platform limestones. Locally, at the top of the
75 Jurassic carbonates a few meters of Lower Cretaceous calcareous-marly deposits are preserved
76 (Carraro et al., 1970).

77 The basement of the Subbriançonnais succession is unknown as it is detached in correspondence of
78 Upper Triassic shales. Above, a thick carbonate succession (200-300 m) of uncertain age (Early-
79 Late Jurassic) is present, and shows the same features as the coeval Provençal interval. The
80 Cretaceous succession is characterized by important lateral variations: it is absent in the south-
81 eastern sector (Bec Matlas, Fig. 1), while it reaches thicknesses of one hundred meters in the north-
82 western sector (M. Pianard, Fig. 1). Here, it is formed by bioclastic limestones, probably of Early
83 Cretaceous age, and by Upper Cretaceous marly limestones and sandy limestones (Zappi, 1960).

84 In both Provençal and Subbriançonnais units, the top of the Mesozoic succession is truncated by a
85 regional unconformity corresponding to a hiatus spanning the Late Cretaceous-Middle Eocene.
86 Above the unconformity, the Alpine Foreland Basin succession consists of the Middle Eocene
87 Nummulitic Limestone, followed by the hemipelagic Upper Eocene *Globigerina* Marl and by the
88 Upper Eocene-Lower Oligocene turbidite succession of the Grès d'Annot (Sinclair, 1997).

89 The tectonic history of the above described succession was marked in Mesozoic times by syn-
90 sedimentary extensional and strike-slip tectonics (Bertok et al., 2011; 2012). Since Late Eocene-
91 Early Oligocene the paleo-European continental margin was then progressively involved in the on-
92 going formation of the Alpine belt. All the study successions underwent at least three deformation
93 events well recorded at regional scale, firstly with outward (SW) brittle-ductile thrusting and
94 superposed foldings, NE back-vergent folding and then with S-ward brittle thrusting and flexural
95 folding. The overall regional kinematic was displayed in a transpressional regime with important
96 strain partitioning of contractional vs. strike-slip related structural associations (Piana et al., 2009),
97 as evidenced by the occurrence of a post-Oligocene NW-SE Alpine transcurrent shear zone
98 (Limone Viozene Zone, LIVZ) extending for several kilometres from Tanaro valley to the study

99 area. The LIVZ dies out NW-ward some kilometers south of Gesso Valley where it merges with
100 the E-W strike-slip shear zone system known as “Stura Fault” of Ricou and Siddans (1986). Despite
101 the high amount of finite deformation in the study area, strain partitioning allowed preservation of
102 most of the primary stratigraphic features and geometrical relationships.

103 The occurrence of dolomitization affecting the Jurassic limestones of both Provençal and
104 Subbriançonnais units in the study area was already reported, although very briefly, by previous
105 authors (Campanino Sturani, 1967; Carraro et al., 1970; Malaroda, 1970). However, no description
106 of the stratigraphic and petrographic features of the dolomitized sediments was given and no
107 explanation was proposed regarding their genetic processes.

108

109 **3. Methods**

110

111 Field work and geological mapping were performed in order to reconstruct the geometry, extension
112 and distribution of the dolomitized bodies. Petrographic studies were carried out on selected
113 samples by optical microscopy and cathodoluminescence aimed to distinguish different dolomite
114 generations. Fourteen microdrilled samples were measured for their carbon and oxygen isotope
115 composition following the method after McCrea (1950) in which carbonate powder is reacted in
116 vacuum conditions with 99% ortho phosphoric acid at 25 °C (time of reaction: 4 h for calcite and 6–
117 7 h for dolomite) using a Finnigan MAT 252 mass spectrometer (MARUM Stable Isotope
118 Laboratory, Bremen, Germany). The isotopic ratios are expressed as $\delta^{13}\text{C}$ and $\delta^{18}\text{O}$ per mil values
119 relative to the VPDB standard (precision $\pm 0.05\%$). Petrography and microthermometry of primary
120 fluid inclusion assemblages on saddle dolomite were performed, using a Linkam THMSG600
121 heating-freezing stage coupled with an Olympus polarizing microscope (100x objective) at the
122 Department of Earth Sciences, University of Torino (Italy), in order to record the homogenization
123 temperatures.

124

125 **4. Host rocks**

126

127 The studied dolomite occurs mainly within the Jurassic limestones of both Provençal and
128 Subbriançonnais units; locally, however, it also affects tectonic slices of Middle Triassic peritidal
129 carbonates present in the LVDZ. The Jurassic limestones are organized in ill-defined dm- to m-
130 thick beds and mainly consist of mudstones to packstones with echinoderm fragments; the upper
131 portion is made up of bioclastic limestones, ranging from packstones to rudstones and boundstones,

132 rich in corals, nerineid gastropods, thick-shelled bivalves, and stromatoporoids. The
133 stratigraphically highest dolomitized beds are locally represented by lagoonal charophyte-rich
134 wackestones. The lower portion of the dolomitized succession was attributed to the Middle-Upper
135 Jurassic (Carraro et al., 1970), whereas the upper part was dated to the Kimmeridgian-Tithonian by
136 Campanino Sturani (1967). However, lagoonal charophyte-rich beds analogous to those observed in
137 the study area, are reported in the same stratigraphic position in the Provençal successions of the
138 Nice Arc, and are dated to the middle-late Berriasian (Dardeau and Pascal, 1982). At present, the
139 study of the charophyte associations is in progress, in order to verify the possible Berriasian age of
140 the top of the dolomitized limestones.

141

142 **5. Dolomite features**

143

144 Dolomitization shows a great variability in the study area. Some Jurassic limestones are only partly
145 dolomitized with development of scattered crystals with euhedral habits (planar-e fabric of Sibley
146 and Gregg, 1987) (Pl.1A). In other cases dolomitization is more intense and follows a more or less
147 complex network of randomly oriented veins (100 μm - to 2 mm-thick on average) (Pl.1A, B). Veins
148 locally are more closely spaced and arranged along sub-vertical, cm- to dm-wide, zones. No
149 significant geometric relations with the main macroscale Alpine tectonic features (such as faults,
150 master joints or hinge zone of flexural folds) have been observed. Dolomite veins crosscut the
151 bedding and are displaced by younger calcite vein system of tectonic origin. Cm-wide, subvertical
152 tabular bodies of dolomite-cemented breccias with partially dolomitized limestone angular clasts
153 also occur (Pl.1B). Mm- to cm-sized irregularly shaped cavities are geopetally filled up with a basal
154 fine-grained dolomite sediment and by coarse dolomite and calcite cements (Pl.1C) and are
155 interpreted as the result of localized dissolution of the enclosing limestone. Fully dolomitized rocks,
156 with a complete obliteration of primary fabrics, occur as small (dm- to m-wide) masses randomly
157 distributed within the partially dolomitized limestones and show a variety of structures documenting
158 complex transformations. Three most representative types can be recognized:

159 Type 1: Quite homogeneous finely to medium crystalline dolostones, resulting from pervasive
160 replacement of the Jurassic limestones.

161 Type 2: Clast-supported breccias made up of clasts of type 1 dolostones (Pl.1D). Clasts range from
162 centimetric to decimetric in size, subrounded to angular in shape. Locally, angular clasts show a
163 jigsaw puzzle arrangement. The voids between the clasts are filled up with mm-thick rims of a
164 coarsely and very coarsely crystalline (up to a few millimetres) whitish dolomite cement, followed
165 by a dark sparry calcite cement plugging the remaining pores.

166 Type 3: Clast-supported breccias, entirely composed of mm- to cm-long and 100 μm - to 2 mm-
167 wide, plate-like, clasts of medium to coarsely crystalline dolomite, strongly resembling the veins
168 crosscutting the host limestones. The voids between the clasts are filled up with a dark sparry
169 calcite cement.

170 Dolomitization, both partial and complete, crosscuts the host limestone bedding. It affects discrete
171 rock masses that are randomly distributed, and is not constrained to specific stratigraphic intervals.
172 From a microscopic point of view, two dolomite types may be distinguished. One is finely to
173 medium-crystalline, non planar to planar-s (Sibley and Gregg, 1987), inclusion-rich, and occurs
174 only as replacive dolomite. It shows a moderate, purple-red cathodoluminescence. The second type
175 is coarsely- to very coarsely-crystalline, and shows the typical features of saddle dolomite (curved
176 crystal faces, sweeping extinction) (Pl.1C). The alternation of more and less inclusion-rich bands
177 outlines different growth stages. A well-defined zonation is also recognizable in
178 cathodoluminescence: a moderate purple-red zone is followed by a non-luminescent zone with thin
179 red hairlines, in turn overlain by a second moderate purple-red zone. It occurs both as replacive and
180 as void-filling dolomite, the latter giving rise to mm-thick rims fringing dissolution cavity walls and
181 breccia clasts.

182 O isotopes of both dolomite types show values ($\delta^{18}\text{O}$ ranging from -4 to -6 ‰ PDB: Fig. 2) clearly
183 more negative than seawater for dolomitizing fluids. More indicative data come from
184 microthermometric analyses of a selection of primary fluid inclusions on saddle dolomite. Although
185 this study is still in progress and it has not been conducted systematically on all the samples, more
186 than 30 homogenization temperatures measured on a selection of 4 samples, show a relatively tight
187 distribution, ranging from 170 to 220 °C, with the highest frequency around 200 °C. The
188 determination of the fluid salinity has not been possible so far because of the small diameter of the
189 fluid inclusions (few micrometers), that make difficult the observation of the complex phase
190 transitions during freezing and melting of the fluid.

191

192

193 **6. Reworked dolomite**

194

195 The base of the Middle Eocene Nummulitic Limestone, resting on the regional unconformity, is
196 locally represented by a m-thick bed of clast-supported conglomerate with dm-sized clasts of
197 limestones and coarsely crystalline dolomites. The conglomerate is followed by a several m-thick
198 succession of dm-thick normally graded beds, made up of conglomerates to arenites; clasts and
199 grains consist of dolomitic rocks and dolomite crystal fragments (Fig. 3). Clasts commonly show

200 bivalve borings. Petrographic features of clasts and grains clearly document that they represent
201 fragments of the underlying dolomitized limestones.

202 The occurrence of dolomitic clasts in the lower portion of the Nummulitic Limestone was already
203 reported by Campredon (1977) who, however, did not recognize their provenance from the
204 dolomitized Jurassic succession.

205

206 **7. Discussion and conclusions**

207

208 *7.1. Age of dolomitization*

209

210 Although no direct dating is available, timing of dolomite formation is well constrained by
211 undisputable stratigraphic evidence. The age of the youngest dolomitized sediments documents that
212 dolomitization cannot be older than Kimmeridgian-Tithonian (Campanino Sturani, 1967) or even
213 Berriasian on the basis of the newly recognized charophyte-rich beds.

214 The occurrence of clasts and grains of the dolomitized limestones within the basal levels of the
215 Nummulitic Limestone, conversely, states that dolomitization cannot be younger than the Bartonian
216 as indicated by the *Nummulites* association usually found in the Nummulitic Limestone
217 (Campredon, 1977; Varrone and Decrouez, 2007). More precise data come from the observation of
218 Cretaceous sediments of the Provençal Domain in the study area. They are generally referred to the
219 lower Lower Cretaceous (Neocomian: Carraro et al., 1970) and, in none of the limited and scattered
220 outcrops available in the study area, are dolomitized. This allows to further restrict the
221 dolomitization event within the Early Cretaceous

222

223 *7.2. Dolomitization process*

224

225 The geometric (partially dolomitized bodies and dolomite-filled veins crosscutting host limestone
226 bedding), petrographic (saddle dolomite, indicating temperatures higher than about 60 °C; Radke
227 and Mathis, 1980), and geochemical ($\delta^{18}\text{O}$ systematically lower than -4‰ PDB) features of the
228 dolomite, together with preliminary data from primary fluid inclusions (homogenization
229 temperature values around 200 °C), attest that dolomitization took place after the deposition of the
230 whole package of Jurassic limestones, and that dolomitizing fluids were hot and flowed mainly
231 through fractures and veins. Dolomite precipitated both along such fracture systems and replaced,
232 partially or completely, non-fractured volumes of carbonate sediments (type 1 dolostone). This
233 clearly shows that at least part of the host Jurassic limestones were still permeable enough to allow

234 a diffuse flux of dolomitizing fluids. This could suggest that dolomitization took place in an early
235 stage of diagenesis, once again pointing to the Early Cretaceous. In this frame, type 2 dolomite
236 breccias resulted from disruption of fully dolomitized limestones, due to the upward flux of
237 overpressurized fluids whereas type 3 dolomite breccias document a thorough dissolution of a
238 veined host limestone and the consequent collapse of the isolated dolomite vein fills.

239 In order to reconstruct the diagenetic environment of such dolomitization, the burial history of the
240 Jurassic limestones must be taken into account. The occurrence of reworked dolomite clasts,
241 commonly bored, within the basal Nummulitic Limestone interval clearly documents that in the
242 Bartonian the Jurassic limestones, already dolomitized, were exposed on rocky coasts where they
243 could be colonized by endolithic organisms and eroded. Cretaceous to Lutetian sediments are
244 missing or very thin all over the study area. Moreover, they are completely missing as clasts in
245 basal Eocene conglomerates, and the underlying unconformity is never associated to evident
246 angular geometrical relationships. All these lines of evidence lead to conclude that if a Cretaceous-
247 Lutetian sediment package had been deposited on top of the Jurassic limestones, it was surely thin
248 enough as to be removed without leaving any trace before the Bartonian transgression. Further to
249 the NW, at the north-western edge of the Argentera Massif, a Turonian unconformity, associated
250 with slump-scars and chaotic deposits and covered by platform-derived redeposited limestones of
251 late Turonian to Campanian age, is known in literature within the basinal Calcari del Puriac
252 (Sturani, 1962; Carraro et al., 1970; Bersezio et al., 2002). This documents different kinds of
253 erosional processes (gravity sliding and platform shedding) during the Late Cretaceous. However,
254 in coeval basinal sediments, cropping out close to the study area, no evidence of these phenomena
255 occurs, which supports the hypothesis of the substantial primary absence of Cretaceous sediments in
256 the studied successions. A very shallow burial environment can thus be argued for the Jurassic
257 limestones at the time of their dolomitization.

258 From the foregoing considerations it follows that the dolomitizing fluids were at a significantly
259 higher temperature than the ambient temperature of the host rocks, and thus they can be considered
260 true hydrothermal fluids (*sensu* Machel and Lonnee, 2002; Davies and Smith, 2006). The spatial
261 arrangement of the vein network, the occurrence of the breccia bodies, and their features point to a
262 hydrothermal system characterized by several dolomitization pulses separated by hydrofracturing
263 processes. The latter were due to the abrupt expulsion of overpressured fluids raising up along main
264 fluid-flow pathways, likely represented by high-angle faults and related fracture systems. Hydraulic
265 fracturing was commonly associated to dissolution of the host limestone (documented by geopetally
266 filled cavities and type 3 breccias) and followed by dolomite precipitation (cementation of veins and
267 cavities and replacement of the host limestone). This suggests that fluid composition was

268 undersaturated with respect to calcite and oversaturated with respect to dolomite. If the overall picture
269 of a superficial hydrothermal system is supported by field and laboratory data, further geochemical
270 analyses are required in order to better define origin, composition and evolution through time of the
271 dolomitizing fluids and to understand what caused precipitation of the sparry calcite cement which
272 represents the last stage of filling of the still open pores.

273

274 *7.3. Regional implications*

275

276 The recognition of the described dolomite bodies has also important regional implications.
277 Hydrothermal dolomitization indirectly documents a fault activity during the Cretaceous roughly
278 along the transition zone between the Ligurian Briançonnais and the Provençal Domains. Structural
279 and stratigraphic evidence of tectonic activity since Early Cretaceous has been indeed recognized in
280 the adjacent External Ligurian Briançonnais Domain (Bertok et al., 2012), where approximately
281 coeval, although less intense, dolomitization processes are known (Bertok, 2007).

282

283

284 **7. Acknowledgments**

285

286 The authors thank Simona Ferrando (Dipartimento di Scienze della Terra, Università di Torino) for
287 guidance and assistance in fluid inclusion microthermometry. Thierry Dumont and an anonymous
288 reviewer provided useful suggestions which improved the manuscript. A financial contribution by
289 Italian Association for Sedimentary Geology (GeoSed) to L. Barale (2011) is kindly acknowledged.

290

291

291 **References**

292

293 Bersezio R., Barbieri P., Mozzi R., 2002. Redeposited limestones in the Upper Cretaceous
294 succession of the Helvetic Argentera Massif at the Italy-France border. *Eclogae geol. Helv.*, 95, 15-
295 30.

296 Bertok C., 2007. Evidenze di tettonica sinsedimentaria nella successione meso-cenozoica del
297 Brianzese Ligure Occidentale. PhD Thesis, Università di Torino, 161 p.

298 Bertok C., Martire L., Perotti E., d'Atri A., Piana F., 2012. Kilometre-scale palaeoscarpments as
299 evidence for Cretaceous synsedimentary tectonics in the External Briançonnais domain (Ligurian
300 Alps, Italy). *Sediment. Geol.*, 251-252, 58–75.

301 Campanino Sturani F., 1967. Sur quelques Nérinées du Malm des Alpes Maritimes (couverture
302 sédimentaire de l'Argentera et écaillés charriées du Col de Tende). Rendiconti Acc. Naz. Lincei, 8,
303 42, 527-529.

304 Campredon R., 1977. Les Formations Paléogènes des Alpes-Maritimes franco-italiennes. Mém.
305 H.S. Soc. Géol. France, 9, Paris, 199 p.

306 Carraro F., Dal Piaz G.V., Franceschetti B., Malaroda R., Sturani C., Zanella E., 1970. Note
307 Illustrative della Carta Geologica del Massiccio dell'Argentera alla scala 1: 50.000. Mem. Soc.
308 Geol. Ital., IX, 557-663.

309 Dardeau G., Pascal A., 1982. La régression fin-Jurassique dans les Alpes-Maritimes: stratigraphie,
310 faciès, environnements sédimentaires et influence du bâti structural dans l'Arc de Nice. Bulletin du
311 BRGM, (2), I, 3, 193-204.

312 Davies G.R., Smith L.B. Jr., 2006. Structurally controlled hydrothermal dolomite reservoir facies:
313 An overview. AAPG Bull., 90, 11, sp. issue, 1641-1690.

314 Machel H.G., 2004. Concepts and models of dolomitization: a critical reappraisal. In: Braithwaite
315 C.J.R., Rizzi G., Darke G. (Eds.), The geometry and petrogenesis of dolomite hydrocarbon
316 reservoirs. Geol. Soc. London, Sp. Pub., 235, pp. 7-63.

317 Machel H.G., Lonnee J., 2002. Hydrothermal dolomite-a product of poor definition and
318 imagination. Sediment. Geol., 152, 163-171.

319 Malaroda R., 1970. Carta Geologica del Massiccio dell'Argentera alla scala 1: 50.000. Mem. Soc.
320 Geol. Ital., IX.

321 McCrea J.M., 1950. On the isotopic chemistry of carbonates and paleotemperature scale. J. Chem.
322 Phys., 18, 849-857.

323 Molli G., Crispini L., Malusà M.G., Mosca P., Piana F., Federico L., 2010. Geology of the Western
324 Alps-Northern Apennine junction area: a regional review. In: Beltrando M., Peccerillo A., Mattei
325 M., Conticelli S., Doglioni C. (Eds.), The Geology of Italy: tectonics and life along plate margins.
326 Journal of the Virtual Explorer, 36, 10.

327 Piana F., Musso A., Bertok C., d'Atri A., Martire L., Perotti E., Varrone D., Martinotti G., 2009.
328 New data on post-Eocene tectonic evolution of the External Ligurian Briançonnais (Western
329 Ligurian Alps). It. J. Geosciences, 128, 2, 353-366.

330 Radke B.M., Mathis R.L., 1980. On the formation and occurrence of saddle dolomite. J. Sediment.
331 Res., 50, 1149-1168.

332 Ricou L.E., Siddans A.W.B., 1986. The Western Alps. In: Coward M.P., Ries A.C. (Eds.), Collision
333 Tectonics. Geol. Soc. Spec. Publ., 19, 229-244.

334 Sibley D.F., Gregg J.M., 1987. Classification of dolomite rock textures. *J. Sediment. Petrol.*, 57, 6,
335 967-975.

336 Sinclair H.D., 1997. Tectonostratigraphic model for underfilled peripheral foreland basins: an
337 Alpine perspective. *GSA Bull.*, 109, 3, 324-346.

338 Sturani C., 1962. Il complesso sedimentario autoctono all'estremo nord-occidentale del Massiccio
339 dell'Argentera (Alpi Marittime). *Mem. Ist. Geol. Min. Univ. Padova*, XXII, 206 p.

340 Tucker M.E., Wright V.P., 1990. Carbonate sedimentology. Blackwell Science, Oxford, UK, 482 p.

341 Varrone D., Decrouez D., 2007. Eocene larger foraminiferal biostratigraphy in the southernmost
342 Dauphinois Domain (Maritime Alps, France-Italy border). *Riv. It. Paleont. Strat.*, 113, 2, 257-267.

343 Zappi L., 1960. Il Cretaceo subbrianzonese dell'alta Val Grande (Alpi Marittime). *Acc. Naz. Lincei*,
344 *Rendiconti Sc. fis. mat. e nat.*, 8, 28, 876-882.

345
346

347 **FIGURE CAPTIONS**

348 Fig. 1. Geological sketch map of the study area, with three simplified stratigraphic logs of the
349 Subbriançonnais and Provençal Units. (SB = Subbriançonnais; P.-L. Units = Piemonte-Liguria
350 Units).

351 Fig. 1. Schéma géologique du secteur étudié, avec trois successions stratigraphiques simplifiées des
352 Unités Subbriançonnaises et Provençales. (SB = Subbriançonnais; P.-L. Units = Unités Liguro-
353 Piémontaises).

354
355

356 Pl. 1. A. Hand specimen of the Jurassic limestones showing different degrees of dolomitization.
357 The left portion is only partly dolomitized with euhedral scattered crystals of dolomite; the right
358 portion is fully dolomitized, whereas in the middle portion dolomitization follows a network of
359 veins. B. Upper portion of the partially dolomitized Jurassic limestones: note the juxtaposition of
360 cm-wide bands of rock with randomly oriented dolomite-cemented veins and of subvertical tabular
361 bodies of dolomite-cemented breccias. C. Photomicrograph of a cavity filled up with a rim of saddle
362 dolomite and a sparry calcite cement. Note the curved crystal faces and the well-defined zonation of
363 the saddle dolomite coarse crystals. D. Clast-supported breccia with fully dolomitized clasts coated
364 by a mm-thick rim of whitish dolomite cement. Remaining voids are plugged by a sparry, grey to
365 black, calcite cement. Pencil tip for scale, on the left, is 1.5 cm long.

366 Pl. 1. A. Échantillon de calcaire jurassique montrant différents degrés de dolomitisation. La partie
367 gauche est seulement partiellement dolomitisée, avec des cristaux euhédraux dispersés de dolomite;

368 la partie droite est entièrement dolomitisée, tandis que dans la partie centrale la dolomitisation suit
369 un réseau de veines. B. Partie supérieure des calcaires jurassiques partiellement dolomitisés: noter
370 la juxtaposition, à l'échelle centimétrique, de bandes de roche avec réseaux de veines dolomitiques
371 diversement orientées et de corps tabulaires de brèches à ciment dolomitique. C. Vue en lame mince
372 d'une cavité bordée d'un ciment de dolomite en selle et remplie d'un ciment calcitique. Noter les
373 faces courbes des cristaux de dolomite en selle et leur zonage. D. Brèche à support clastique avec
374 clastes entièrement dolomitisés et revêtus d'une frange millimétrique de ciment dolomitique
375 blanchâtre. Les vides résiduels sont remplis d'un ciment de calcite sparitique, de couleur grise à
376 noire. La pointe de crayon sur la gauche mesure 1,5 cm de longueur.

377

378 Fig. 2. $\delta^{18}\text{O}$ versus $\delta^{13}\text{C}$ crossplot of pore-filling calcite (empty squares) and saddle dolomite (black
379 dots). As a term of comparison, dolomites formed at surface in marine environments display
380 isotopic values ranging approximately from +1 to +3 ‰ VPDB for both $\delta^{18}\text{O}$ and $\delta^{13}\text{C}$ (Tucker &
381 Wright, 1990).

382 Fig. 2. Graphique combinée avec les rapports $\delta^{18}\text{O}$ et $\delta^{13}\text{C}$, mesurés sur la calcite (carrés vides) et la
383 dolomite en selle (points noirs) de remplissage des pores. Pour comparaison, la dolomite formée à
384 la surface dans des environnements marines montre des valeurs isotopiques compris entre +1 to +3
385 ‰ VPDB environ pour $\delta^{18}\text{O}$ et $\delta^{13}\text{C}$ (Tucker & Wright, 1990).

386

387

388 Fig. 3. Conglomerate bed in the lower part of the Nummulitic Limestone, with mm- to cm-sized
389 clasts of dolomitized rocks.

390 Fig. 3. Niveau conglomératique dans la partie inférieure des Calcaires Nummulitiques, contenant
391 des galets dolomitisés millimétriques à centimétriques.

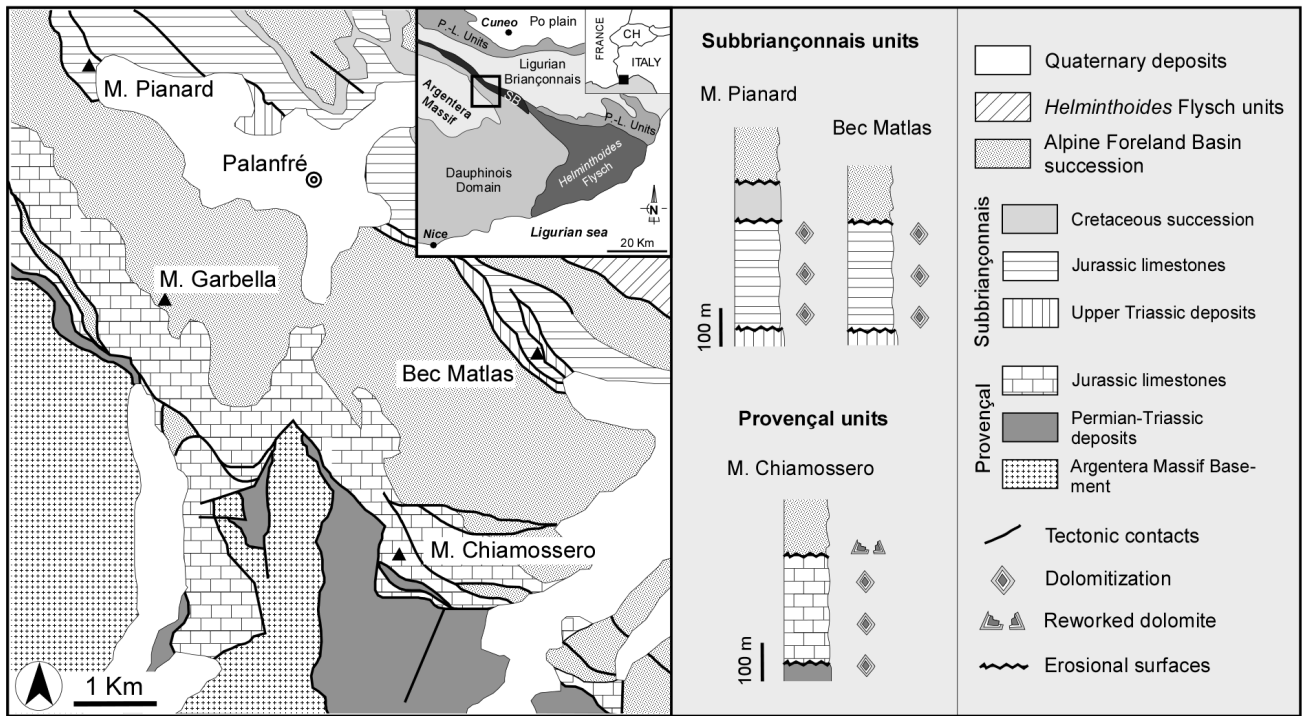
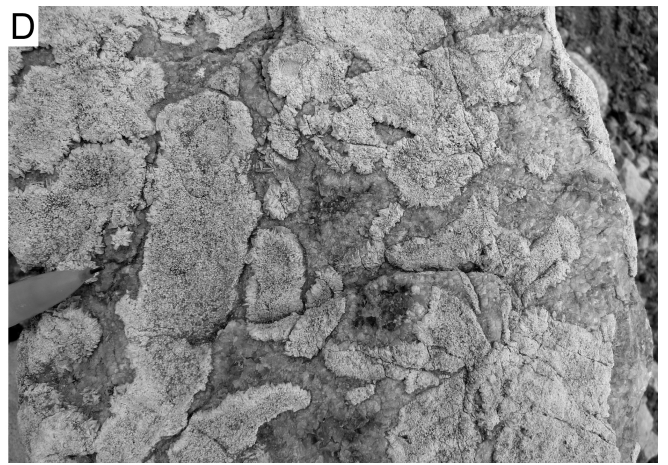
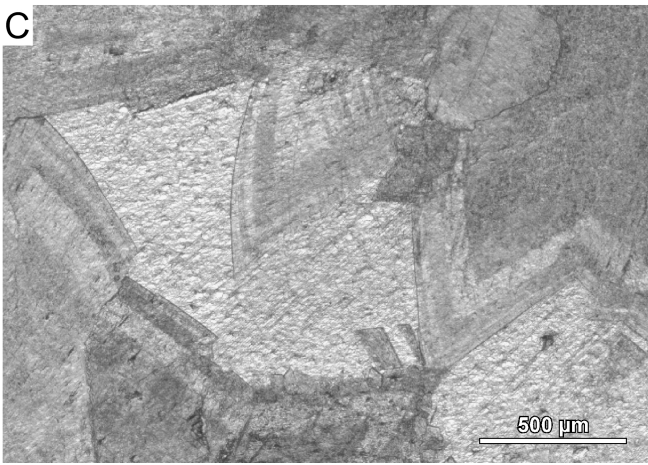
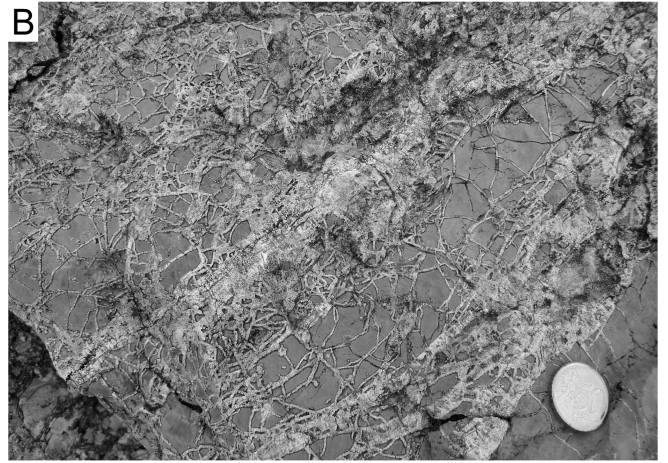
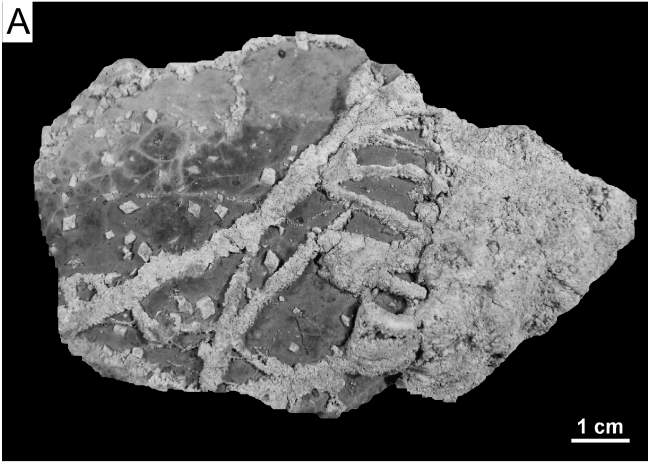


Fig. 1.



Pl. 1.

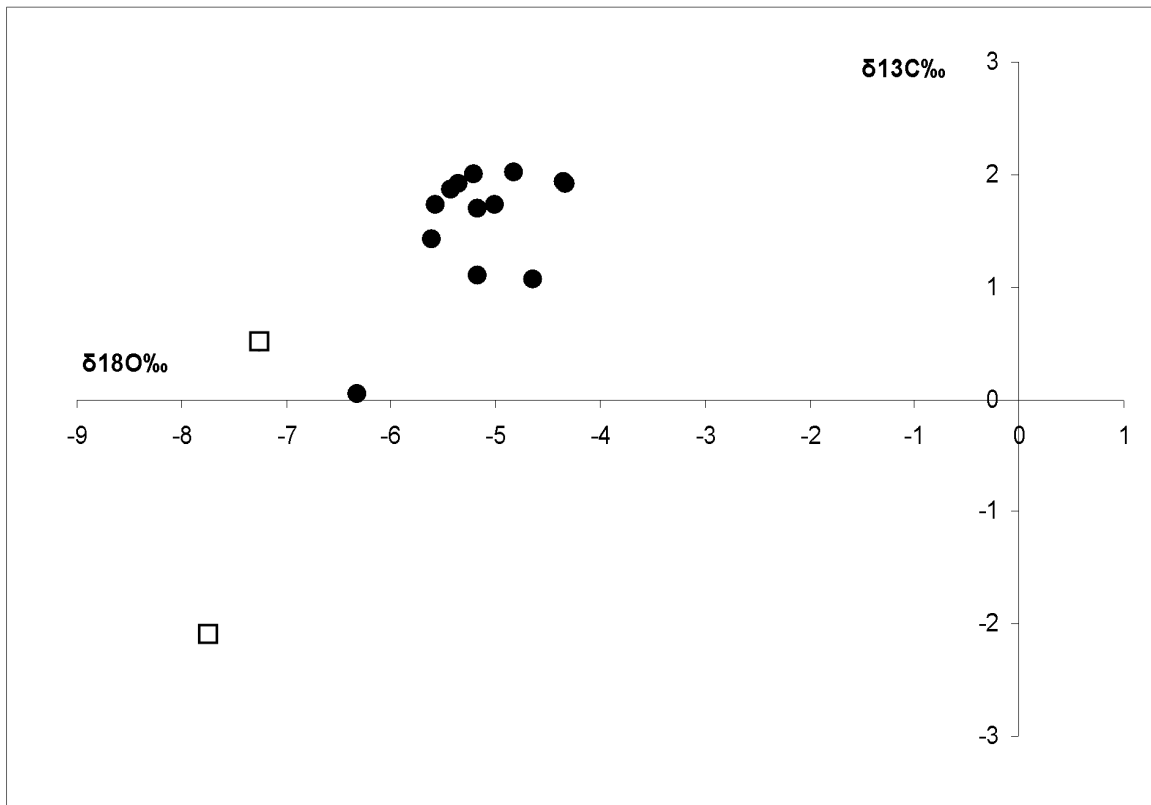


Fig. 2.



Fig. 3.